Coordination entities of a Pyrene-based Iminopyridine ligand: Structural and photophysical properties

Awatef Ayadi, Diana-G. Branzea, Magali Allain, David Canevet, Haluk Dincalp, Abdelkrim El-Ghayoury

▶ **To cite this version:**

Awatef Ayadi, Diana-G. Branzea, Magali Allain, David Canevet, Haluk Dincalp, et al.. Coordination entities of a Pyrene-based Iminopyridine ligand: Structural and photophysical properties. Polyhedron, 2017, 135, pp.86-95. 10.1016/j.poly.2017.07.001 . hal-02564433

HAL Id: hal-02564433

https://univ-angers.hal.science/hal-02564433

Submitted on 5 May 2020

HAL is a multi-disciplinary open access archive for the deposit and dissemination of scientific research documents, whether they are published or not. The documents may come from teaching and research institutions in France or abroad, or from public or private research centers.

L'archive ouverte pluridisciplinaire **HAL**, est destinée au dépôt et à la diffusion de documents scientifiques de niveau recherche, publiés ou non, émanant des établissements d'enseignement et de recherche français ou étrangers, des laboratoires publics ou privés.

Accepted Manuscript

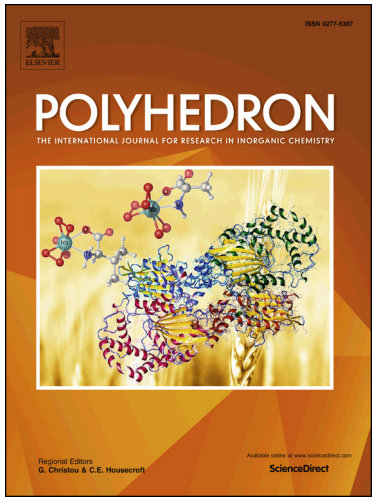

Coordination entities of a Pyrene-based Iminopyridine ligand: Structural and photophysical properties

Awatef Ayadi, Diana G. Branzea, Magali Allain, David Canevet, Haluk Dinçalp, Abdelkrim El-Ghayoury

PII: S0277-5387(17)30483-7
DOI: http://dx.doi.org/10.1016/j.poly.2017.07.001
Reference: POLY 12736

To appear in: *Polyhedron*

Received Date: 13 March 2017
Revised Date: 30 June 2017
Accepted Date: 1 July 2017

Please cite this article as: A. Ayadi, D.G. Branzea, M. Allain, D. Canevet, H. Dinçalp, A. El-Ghayoury, Coordination entities of a Pyrene-based Iminopyridine ligand: Structural and photophysical properties, *Polyhedron* (2017), doi: http://dx.doi.org/10.1016/j.poly.2017.07.001

This is a PDF file of an unedited manuscript that has been accepted for publication. As a service to our customers we are providing this early version of the manuscript. The manuscript will undergo copyediting, typesetting, and review of the resulting proof before it is published in its final form. Please note that during the production process errors may be discovered which could affect the content, and all legal disclaimers that apply to the journal pertain.

ACCEPTED MANUSCRIPT

Coordination entities of a Pyrene-based Iminopyridine ligand: Structural and photophysical properties

Awatef Ayadi,[a,b] Diana G. Branzea,[a] Magali Allain,[a] David Canevet,[a] Haluk Dinçalp,[c] Abdelkrim El-Ghayoury[a]*

[a] *Université d'Angers, CNRS UMR 6200, Laboratoire MOLTECH-Anjou, 2 bd Lavoisier, 49045 Angers Cedex, France.*
Email: abdelkrim.elghayoury@univ-angers.fr, Phone: +33 (0) 241735492, Fax: +33 (0) 241735405.
[b] *Laboratoire de Physico-Chimie de l'Etat Solide, Université de Sfax, Route de Soukra; Km 4; BP: 802, 3038, Sfax, Tunisia.*
[c] *Department of Chemistry, Faculty of Arts and Science, Celal Bayar University, 45030 Muradiye-Manisa, Turkey.*

Abstract

A pyrene-based iminopyridine ligand **L** has been prepared and displays the absorption and emission properties expected for pyrene-based derivatives in solution. Ligand **L**, as well as two neutral and one monocationic coordination entities, respectively formulated as [$ZnLCl_2$] **1**, [$ReLCl(CO)_3$] **3** and [CuL_2](BF_4) **2**, have been crystallized and analyzed by single crystal X-ray diffraction analysis. The corresponding crystal structures indicate the formation of supramolecular architectures generated by offset $\pi\cdots\pi$ stacking between pyrene fragments and strong C–H$\cdots\pi$ interactions in coordination entity **1**. For the cationic coordination entity **2**, the crystal packing reveals the presence of C–H$\cdots$F and C–H$\cdots\pi$ interactions and numerous C–H$\cdots\pi$ contacts interconnecting the molecules into a 3D network. As for coordination entity **3**, hydrogen bonding and $\pi\cdots\pi$ stacking link the molecules in a three dimensional manner. Zinc (II) and copper (I) coordination entities have also been studied through isothermal titration calorimetry, which indicate a strong binding and a different stoichiometry for both coordination entities. Photophysical studies of the ligand and corresponding coordination entities show a monomer type pyrene emission and a higher fluorescence quantum yield for the zinc coordination entity **1** as compared with copper **2** and rhenium **3** coordination entities.

ACCEPTED MANUSCRIPT

1. Introduction

Pyrene, the smallest peri-fused polycyclic aromatic hydrocarbon, was first isolated in the mid-19th century from coal tar[1] and is usually obtained during the combustion of organic compounds.[2] This unit is widely exploited for its electronic and photophysical properties, and for its ability to take part in non-covalent interactions.[3] It has found use as active material for organic electronics applications such as OFETs, OLEDs and more recently as donor component in organic solar cells (OSCs).[4] In addition, pyrene has played a major role for the preparation of supramolecular fluorescent chemosensors for charged and neutral species which remains a very active field of research.[5] In fact, pyrene can be regarded as one of the most useful sensing molecules because it may emit as a monomer near 370-380 nm or as an excimer near 480 nm, depending on its environment in the excited state.[6] In particular, on-going research for the design of such fluorescent chemosensors consists in covalently grafting one or multiple fluorophores onto a coordinating unit that can bind metal cations.[7] For example, pyrene-bipyridine ligands and their corresponding coordination entities,[8] pyrene-terpyridine,[9] pyrene-hydroxamate,[10] pyrene-ethynyl[11] and pyrene-salicylidenes have been reported and their photophysical properties investigated.[12] The pyrene unit has been used in combination with nitronylnitroxide and iminonitroxide radicals and their corresponding copper(II) coordination entities in which strong intramolecular copper(II)–radical AFM and FM exchange interaction was observed.[13]

Pyridine containing Schiff bases, such as 2-iminopyridyls form stable coordination entities with various transition metals. For instance, they have been used in metallo-organic self-assembling media to produce discrete metallo-supramolecular helicates,[14] cages[15] and capsules.[16] It is worth mentioning that iron coordination entities of such ligands were employed successfully in catalysis.[17] In addition, these ligands have been used in association with fluorescent subunit as chemosensors for metal ions.**5**[a,18]

Of particular importance, pyridine-based Schiff base ligands can be used to coordinate copper(I) or zinc(II) ions that are essential elements for life and form particularly stable coordination entities with these metals. [19] It is therefore of interest to design ligands that are capable of sensing (by spectroscopic techniques) and ultimately to isolate and characterize the resulting coordination entities. For instance, d^{10} metal coordination entities of Schiff base ligands have been successfully used in co-sensitized solar cells.[20]

ACCEPTED MANUSCRIPT

The following work describes the synthesis of the pyrene-based iminopyridine ligand **L**, which has been reported in the literature during the ongoing of the present work,[17c,21,22,23] and its corresponding Zn(II), Cu(I) and Re(I) transition metal coordination entities which have been structurally characterized using X-ray diffraction analysis. The photophysical behaviors of both ligand and coordination entities have been investigated. In addition, the binding constants of Zn(II) and Cu(I) coordination entities have been determined by means of ITC and/or absorption techniques.

2. Experimental

2.1 General considerations

All the chemicals and solvents were of reagent grade quality and used as received. NMR spectra were recorded on a Bruker Avance DRX 300 spectrometer operating at 300 MHz for ^{1}H and 75 MHz for ^{13}C. Chemical shifts are expressed in parts per million (ppm) downfield from external TMS. Mass spectra were collected with a Bruker Biflex-III TM spectrometer. IR absorption spectra were recorded on a Bruker Vertex 70. UV–vis absorption spectra were recorded using an Analytic Jena Speedcord S-600 diode-array spectrophotometer in solutions. Fluorescence and lifetime measurements were recorded on a FLSP 920 Edinburg fluorescence phosphorescence spectrophotometer. The excitation wavelength was set to 317 nm for solution measurements. Quantum yields of fluorescence were measured by comparing the fluorescence intensity of the sample to that of the optically dilute solutions of pyrene standard. Ligand **L** and coordination entities **1-3** were dissolved in chlorobenzene for solid-state measurement. A thin layer of the compounds was obtained by spin coating at 1500 rpm/s and dried subsequently at 70 °C for 20 min in a vacuum-controlled oven.

2.2 Crystal structure determinations

Experimental X-ray diffraction data on single crystals were collected at room temperature using a Bruker Nonius Kappa CCD diffractometer operating with a Mo-Kα (λ = 0.71073 Å) X-ray tube with a graphite monochromator. The structures were solved by direct methods and refined (SHELXL-97) by full-matrix least-square procedures on F^2.[24] All non-H atoms of the molecules were refined anisotropically, and hydrogen atoms were introduced at calculated positions (riding model), included in structure factor calculations but not

ACCEPTED MANUSCRIPT

refined. Details about data collection and solution refinement are given in Table 1. Crystallographic data for the structural analysis have been deposited within the Cambridge Crystallographic Data Centre, CCDC 1452985 (ligand **L**), CCDC 1012506 (coordination entity **1**), CCDC 1012507 (coordination entity **2**) and CCDC 1012508 (coordination entity **3**).

Table 1. Crystal Data and Structure Refinement for **L**, **1**, **2** and **3**.

compound	Ligand **L**	**1**	**2**	**3**
empirical formula	$C_{22}H_{14}N_2$	$C_{22}H_{14}Cl_2N_2Zn$	$C_{44}H_{28}BCuF_4N_4$	$C_{25}H_{14}ClN_2O_3Re$
fw	306.35	442.62	763.05	612.03
cryst syst	monoclinic	triclinic	monoclinic	orthorhombic
space group	*P* 2_1	*P* -1	*C* 2	*Pcab*
a (Å)	5.044(2)	8.9700(4)	18.9332(15)	9.7256(8)
b (Å)	19.810(9)	9.0556(4)	8.3009(7)	15.5107(14)
c (Å)	15.744(5)	12.1015(8)	11.9498(7)	28.632(3)
α(deg)	90.00	95.046(5)	90.00	90.00
β(deg)	92.92(3)	99.199(5)	107.483(5)	90.00
γ(deg)	90.00	104.687(5)	90.00	90.00
V ($Å^3$)	1571.0(11)	930.10(9)	1791.3(2)	4319.2(7)
Z	4	2	2	8
D_c (g cm^{-3})	1.295	1.580	1.415	1.882
abs coeff (mm^{-1})	0.077	1.616	0.669	5.781
F(000)	640	448	780	2352

ACCEPTED MANUSCRIPT

Crystal size (mm^3)	0.27× 0.04× 0.03	0.25 × 0.2 × 0.15	0.45 × 0.12 × 0.05	0.5 × 0.3 × 0.2
θ range for data collection (deg)	4.02–25.39	3.82–27.51	4.18–27.48	3.87–27.54
reflns collected	10353	17715	17930	17165
indep reflns	4841	4250	3931	4910
completeness (%)	96.6	99.6	99.4	98.6
data/restraints/param	2132/1/433	2318/0/244	2514/15/254	2859/0/289
GOF on F^2	1.004	0.972	1.010	1.030
final R indices [$I > 2\sigma(I)$]	R1 =0.0611, wR2 = 0.0891	R1 = 0.0439, wR2 = 0.0689	R1 = 0.0456, wR2 = 0.0869	R1= 0.0401, wR2 = 0.0483
R indices (all data)	R1 =0.1862, wR2 = 0.1205	R1 = 0.1298, wR2 = 0.0815	R1 = 0.1079, wR2 = 0.0982	R1= 0.1008, wR2 = 0.0583
Absolute structure parameter (Flack)	0.0(10)	-	0.018(7)	-
largest diff. peak and hole (e $Å^{-3}$)	0.179 and –0.163	0.317 and –0.314	0.369 and –0.364	0.751 and –0.635

*2.3. Synthesis of ligand (**L**)*

Preparation of ligand **L** was adapted from the previously reported procedure by us. [25] 1-Aminopyrene (0.150 g, 0.69 mmol) and 2-pyridinecarboxaldehyde (0.070 g, 0.65 mmol) were dissolved in ethanol (20 mL), three drops of acetic acid were added and the reaction mixture was refluxed overnight. After cooling to room temperature, a brown precipitate was formed which was filtered and washed with additional

ACCEPTED MANUSCRIPT

ethanol and dried to afford a yellow powder of ligand **L** (0.152 g, 80 %). ^{1}H-NMR (300 MHz, CD_2Cl_2) δ/ppm: 8.93 (s, 1H), 8.8 (d, 1H, J = 4.8 Hz), 8.76 (d, 1H, J = 9.2 Hz), 8.51 (d, 1H, J = 7.9 Hz), 8.25 (m, 3H), 8.18 (d, 1H, J = 9.2 Hz), 8.11 (d, 2H, J = 1.4 Hz), 8.10-7.94 (m, 2H), 7.91 (d, 1H, J = 8.2 Hz), 7.48 (ddd, 1H, J = 1.1, 4.8 and 7.5). Selected IR bands (cm^{-1}): $\bar{\upsilon}$ = 1615, 1579, 1563, 1468, 1432, 839. Anal. Calc. for $C_{22}H_{14}N_2$: C, 86.25 %; H, 4.61 %; N, 9.14 %. Found: C, 86.09 %; H, 4.43 %; N, 8.86 %. MALDI-TOF MS calcd: m/z = 306.11 Da. Found: m/z = 306.3. HRMS (M) for $C_{22}H_{14}N_2$: 306.1156. Found: 306.1159.

2.3. Synthesis of coordination entity ***(l)***

Ligand **L** (0.020 g, 0.064 mmol) in CH_2Cl_2 (5 mL) was reacted with one equivalent of $ZnCl_2$ (0.009 g, 0.064 mmol) in CH_3CN (3 mL). The mixture was sonicated for 5 min and on top of this solution, diethyl ether was added which led to the formation of single crystals of coordination entity [$ZnLCl_2$] **1** after one week. Yield: 63%. ^{1}H-NMR (300 MHz, CD_2Cl_2) δ/ppm: 9.03 (d, 1H, J = 4.6 Hz), 8.94 (s, 1H), 8.73 (d, 1H, J = 10.0 Hz), 8.36 (d, 5H, J = 7.4 Hz), 8.21 (m, 4H), 8.03 (d, 2H, J = 7.9 Hz). Selected IR bands (cm^{-1}): $\bar{\upsilon}$ = 1594, 1480, 1443, 1024, 837. Anal. Calc. for $C_{22}H_{14}N_2Cl_2Zn$: C, 59.69 %; H, 3.19 %; N, 6.33 %. Found: C, 59.42 %; H, 3.14 %; N, 6.30 %. MALDI-TOF MS calcd: m/z $(M\text{-}Cl)^+$ = 405.01 Da. Found: m/z = 405.3. HRMS $(M\text{-}Cl)^+$ for $C_{22}H_{14}ClN_2Zn$: 405.0136. Found: 405.0133.

2.4. Synthesis of coordination entity ***(2)***

In a test tube, a solution of ligand **L** (0.020 g, 0.065 mmol) in CH_2Cl_2 (5 mL) was mixed with a solution of $Cu(CH_3CN)_4BF_4$ (0.011 g, 0.032 mmol) in CH_3CN (5 mL) and sonicated for 5 min. On top of the resulting solution a layer of diethyl ether was added, which led to the formation of single crystals of coordination entity $[Cu(L)_2]BF_4$ **2** after one week with 92 % Yield. ^{1}H-NMR (300 MHz, CD_2Cl_2) δ/ppm: 8.86 (d, 2H, J = 3.5 Hz), 8.57 (s, 2H), 8.11 (m, 6H), 7.98 (m, 6H), 7.93 (m, 6H), 7.50 (d, 2H, J = 8.1 Hz), 7.38 (d, 2H, J = 9.1 Hz), 6.80 (d, 2H, J = 7.9 Hz). Selected IR bands (cm^{-1}): $\bar{\upsilon}$ = 1593, 1591, 1473, 1440, 1050, 848. Anal. Calc. for $C_{44}H_{28}N_4CuBF_4$: C, 69.26 %; H, 3.70 %; N, 7.34 %.

ACCEPTED MANUSCRIPT

Found: C, 69.65 %; H, 3.63 %; N, 7.41 %. MALDI-TOF MS calcd: m/z ($M-BF_4^-$) = 675.16 Da. Found: m/z = 675.6. HRMS ($M-BF_4^-$) for $C_{44}H_{28}CuN_4$: 675.1609. Found: 675.1612.

2.5. Synthesis of coordination entity ***(3)***

Under nitrogen, a solution of ligand **L** (0.020 g, 0.065 mmol) and $[Re(CO)_5Cl]$ (0.024 g, 0.065 mmol) was heated to reflux for 4 hours in a mixture of toluene and dichloromethane (15 mL; 3/1: v/v). The solvent was removed from the solution and the solid residue was recrystallized from acetone/hexane to yield 85% of orange coordination entity $[ReLCl(CO)_3]$ **3**. ^{1}H-NMR (300 MHz, $CDCl_3$) δ/ppm: 9.22 (d, 1H, J = 4.7 Hz), 9.06 (s, 1H), 8.19 (m, 11H), 7.73 (m, 1H). ^{13}C-NMR (300 MHz, $CDCl_3$) δ/ppm: 169.7, 169.6, 169.5, 155.2, 154.9, 153.5, 144.8, 139.24, 131.4, 131.4, 130.9, 130.8, 129.3, 129.3, 129.2, 128.3, 127.3, 126.7, 126.3, 125.8, 125.7, 125.3, 120.2, 120.1, 120.0. Selected IR bands (cm^{-1}): $\bar{\upsilon}$ = 2014, 1920, 1873, 1591, 1447, 1186, 1158, 840. Anal. Calc. for $C_{25}H_{14}N_2Cl\,O_3Re$: C, 48.82 %; H, 2.79 %; N, 4.55 %. Found: C, 48.65 %; H, 3.32 %; N, 4.49 %. MALDI-TOF MS calcd: m/z ($M-Cl^-$) = 577.05 Da. Found: m/z = 577.1. HRMS ($M-Cl^-$) for $C_{25}H_{14}N_2O_3Re$: 577.0562. Found: 577.0541.

Results and discussion

General synthetic strategy

Ligand **L** was obtained in a good yield by the condensation reaction between 1-aminopyrene and 2-pyridinecarboxaldehyde (Scheme 1). Coordination tests were performed for ligand **L** in order to evaluate its propensity to form coordination entities with transition metals. In fact, the reaction between ligand **L** and zinc chloride ($ZnCl_2$) in a 1:1 ratio yielded the expected monomeric coordination entity of formula $[Zn(L)Cl_2]$ **1**. In order to obtain a homoleptic coordination entity, ligand **L** was reacted with a copper(I) coordination entity $[Cu(CH_3CN)_4]BF_4$ in a 2:1 ratio to afford $[Cu(L)_2]BF_4$ **2**. Unlike previous cases, the equimolar reaction between ligand **L** and the $[Re(CO)_5Cl]$ precursor was performed by refluxing a mixture of toluene and dichloromethane under inert atmosphere, so as to obtain coordination entity **3** as an orange precipitate.[26]

ACCEPTED MANUSCRIPT

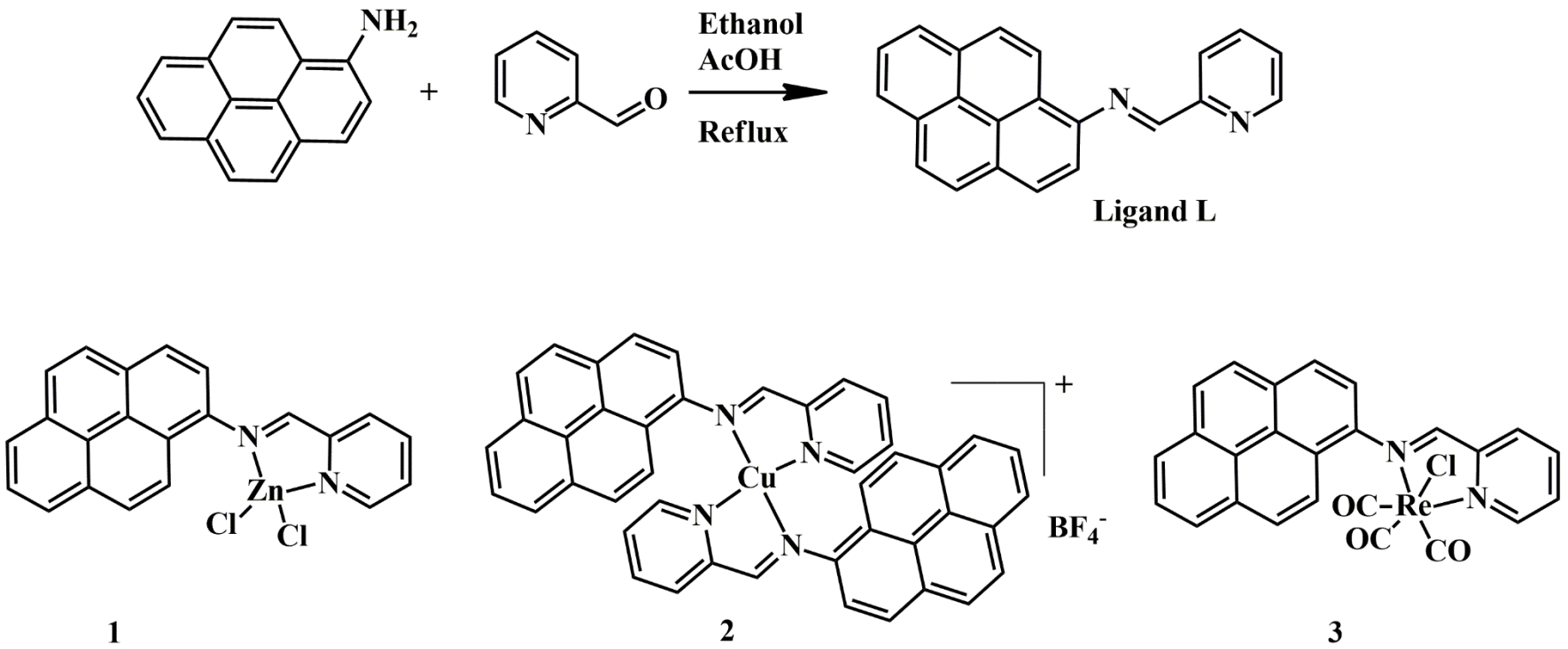

Scheme 1. Synthetic procedure for ligand **L** and chemical structures of coordination entities **1-3**.

Crystal structures description

Suitable single crystals for X-ray analysis have been grown for ligand **L** upon slow evaporation of dichloromethane (DCM) solvent. Ligand **L** crystallizes as brown plates in the monoclinic system, space group $P2_1$, with two independent molecules in the unit cell. Parameters of the single crystal X-ray diffraction studies are gathered in Table 1, selected bond lengths and angles are depicted in Table 2. Within the ligand (figure 1), the dihedral angle between the pyrene fragment and the iminopyridine group is 6.138 (11)°. In the solid state, each ligand molecule interacts with

ACCEPTED MANUSCRIPT

two neighboring ones by hydrogen bonds, C–H···π (C1–H1···C19 (2.805 (6) Å), (C23–H23···C10 (2.890 (5) Å), (C18–H18···C13 (2.864 (5) Å) from pyridine ring and two from pyrene fragment respectively as represented in Figure S1.

In the other hand, each ligand molecule interacts with the adjacent molecule by non-conventional hydrogen bonds C–H···N (C1–H1···N2 (2.625 (5) Å), (C17–H17···N1 (2.845 (5) Å), and (C10–H10···N2 (2.855 (6) Å). These interactions lead to the formation of 2D supramolecular layers parallel with the *bc* crystallographic plane. Within the layer, the molecules stack in parallel infinite columns with an off-set head to head arrangement due to π···π interactions involving, two by two, the aromatic rings of the pyrene from adjacent molecules (centroid···centroid: 3.64 Å).[27] According to Kruszynski *et al*. who suggest that the stacking interactions exist at large Cg...Cg distances (up to 7Å)[28], the ligand forms over 40 specific interactions between the 6-membered rings (Table S1).

ACCEPTED MANUSCRIPT

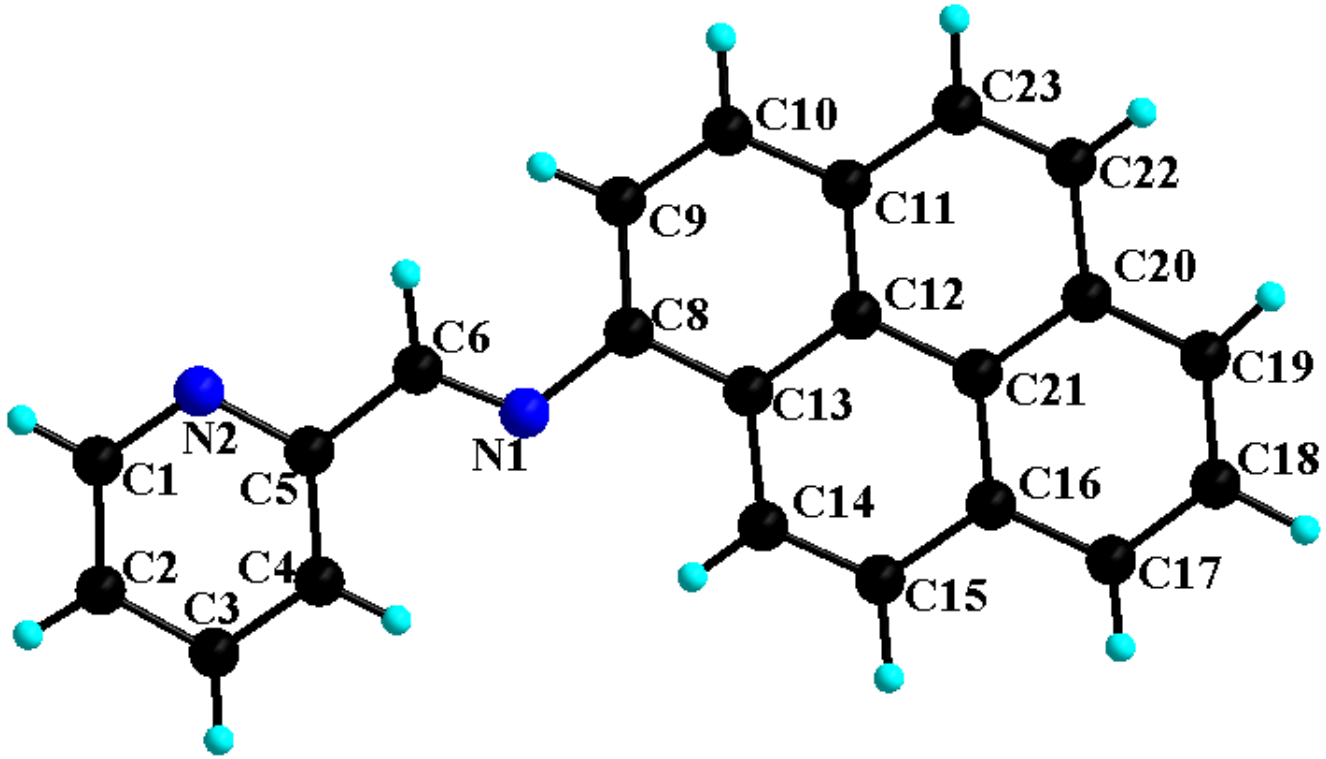

Fig. 1 Crystal structure of ligand **L** with atom numbering scheme.

Single crystals of coordination entity **1** were obtained *via* slow diffusion of diethyl ether into a dichloromethane/acetonitrile mixture, and the crystal structure was determined using single crystal X-ray diffraction analysis confirming the proposed formula of the coordination entity (Fig. 2). The relevant bond and angle parameters are summarized in Table 2.

Table 2. Selected bond lengths (Å) and angles (°) in **L**, **1**, **2** and **3**

ACCEPTED MANUSCRIPT

bond length (Å)							
Ligand **L**		**1**		**2**		**3**	
C5—N2	1.346(8)	C1—N1	1.346(4)	C1—N1	1.355(8)	N1—Re1	2.177(4)
C5—C6	1.470(8)	C5—N1	1.337(4)	C5—N1	1.346(7)	N2—Re1	2.177(4)
C6—N1	1.244(9)	C6—N2	1.281(3)	C6—N2	1.275(7)	Cl1—Re1	2.466(14)
N1—C8	1.425(7)	C7—N2	1.440(4)	C7—N2	1.435(7)	C23—Re1	1.923(6)
angle values (°)		N1—Zn1	2.067(2)	N1—Cu1	2.041(4)	C24—Re1	1.915(6)
N2—C5—C6	115.66(5)	N2—Zn1	2.134(2)	N1—Cu1	2.090(4)	C25—Re1	1.922(7)
C5—C6— N1	122.13(6)	Cl1—Zn1	2.2076(8)	F1—B1	1.354(1)	C6—N2	1.283(6)
C6—N1—C8	121.44(5)	Cl2—Zn1	2.2011(8)	F2A—B1	1.587(1)	C1—C6	1.453(7)
N1—C8—C9	124.40(5)			F2B—B1	1.253(1)		
		angle values (°)					
		N1—Zn1—N2	80.00(9)	N1—Cu1—N1i	118.5(3)	C24—Re1—C026	89.8(3)
		N1—Zn1—Cl2	118.25(7)	N1—Cu1—N2	80.94(18)	C24—Re1—C011	89.4(2)
		N2—Zn1—Cl2	101.22(7)	N1i—Cu1—N2	136.02(16)	C25—Re1—C011	88.7(2)
		N1—Zn1—Cl1	110.82(7)	N1—Cu1—N2i	136.02(16)	C24—Re1—N1	94.0(2)
		N2—Zn1—Cl1	115.08(7)	N1i—Cu1—N2i	80.94(18)	C25—Re1—N1	173.7(2)
		Cl2—Zn1—Cl1	122.71(3)	N2—Cu1—N2i	113.3(2)	C23—Re1—N1	96.3(2)
						C24—Re1—N2	168.1(2)
						C25—Re1—N2	101.8(2)
						C23—Re1—N2	92.83(19)
						N1—Re1—N2	74.21(17)
						C24—Re1—Cl1	93.68(16)

ACCEPTED MANUSCRIPT

	C25—Re1—Cl1	89.48(18)
	C23—Re1—Cl1	176.42(18)
	N1—Re1—Cl1	85.26(12)
	N2—Re1—Cl1	84.50(12)
	O1—C23—Re1	176.2(6)
	O3—C24—Re1	174.5(5)
	O2—C25—Re1	177.7(5)

Symmetry transformation used to generate equivalent atoms for compound **2**: (i) 1-x, y, -z.

ACCEPTED MANUSCRIPT

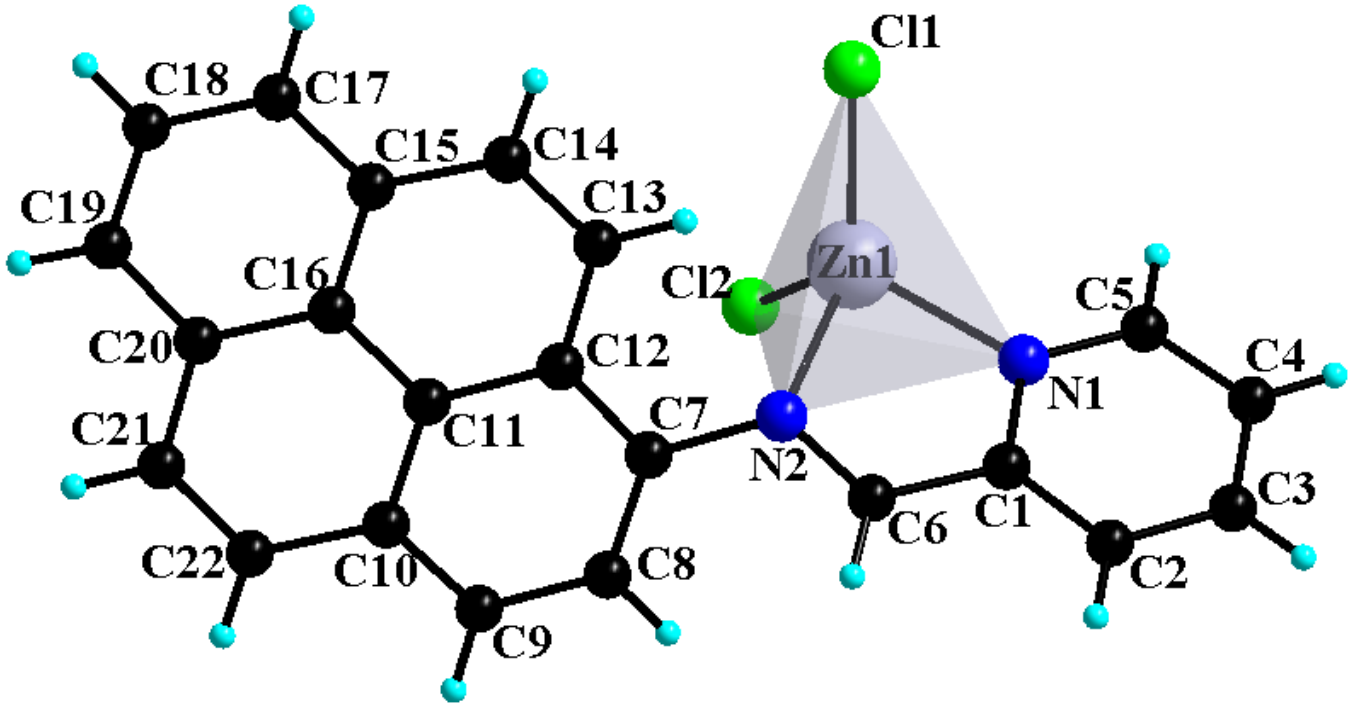

Fig. 2 Crystal structure representation of coordination entity **1** with the atom-numbering scheme.

This coordination entity crystallizes in the triclinic system, space group *P-1*, with one independent molecule in the unit cell. The coordination sphere of the central metal ion is formed by the two nitrogen atoms of the bidentate ligand, **L**, and two chlorine atoms and its geometry can be described as tetrahedral. The different nature of the ligands surrounding the metal cation, namely the bidentate iminopyridyl **L** ligand with a small bite angle (N1–Zn1–N2 80.00(9)°), and two chlorine atoms resulted in a distortion of the tetrahedral environment. As observed in other of zinc coordination entities with similar iminopyridyl type ligands,[29] the Zn1–N1(pyridyl) bond (Zn1–N1 2.067(2) Å) is somewhat shorter than the

ACCEPTED MANUSCRIPT

Zn1-N2(imino) (Zn1–N2 2.134(2) Å) bond. The formal double bond character in the imino fragment is maintained (C6–N2 1.281(3) Å). The Zn1–Cl1 and Zn1–Cl2 bond lengths are 2.2076(8) Å and 2.2011(8) Å, respectively. The dihedral angle between the least-square planes of the pyrene fragment and N,N-iminopyridyl moiety is 56.54°; this value can also be explained by the geometrical restraints of the vicinal chlorine atom.

In the crystal lattice, short C–H···Cl contacts (C–H···Cl: H5···Cl1 2.80 Å, H2···Cl2 2.77 Å) are established by both chlorine atoms with hydrogen atoms from the pyridine rings from neighboring molecules. This results in a supramolecular chain parallel with the crystallographic *a* axis (Fig. S2). Each chain is reinforced by $\pi\cdots\pi$ off-set stacking involving, two by two, the pyridine rings from adjacent molecules (centroid···centroid 3.71 Å). Due to the above-mentioned interactions, the pyrene fragments of each ligand molecule are oriented on the two sides of the chain having a parallel arrangement with a distance between planes of 7.06 Å.

Furthermore, viewing along the crystallographic *b* axis, weak offset $\pi\cdots\pi$ stacking between the aromatic rings of the adjacent pyrene units (the pyrene fragments overlap only partially, the centroid···centroid distances varying from 3.69 Å to 3.77 Å) and also a C–H$\cdots\pi$ interaction between one aromatic ring of the pyrene (C15÷C20) unit and the adjacent N═CH hydrogen atom (H6···centroid 2.77 Å) are observed. These interactions actually act as a zipper to join the neighboring chains into a supramolecular layer (Fig. S3). As for ligand L, coordination entity 1 forms over 40 specific interactions between the 6-membered rings[28] (Table S2).

Employing the same crystallization technique, namely slow diffusion, single crystals of coordination entity $[Cu(L)_2]BF_4$ **2** were grown and, thus crystal structure investigations were pursued and confirmed our expectations. coordination entity **2** was found to crystallize in the monoclinic system, *C*2 space group, with half of the coordination entity cationic unit, $[Cu(L)_2]^+$, and half of the uncoordinated BF_4^- anion (Fig. 3). Parameters of the single crystal X-ray diffraction studies are gathered in table 1.

ACCEPTED MANUSCRIPT

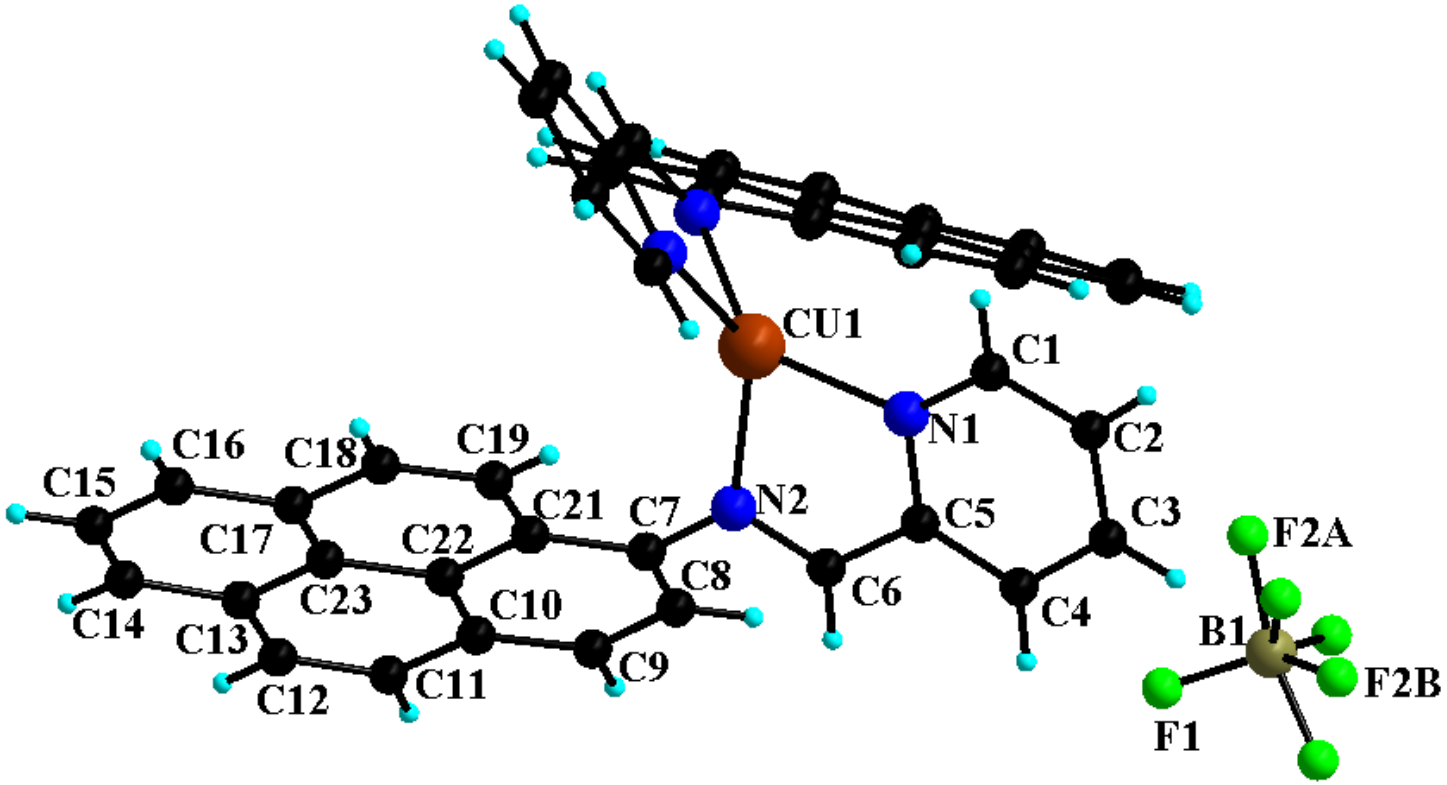

Fig. 3 Crystal structure of coordination entity **2** with the atom-numbering scheme.

Within the monocationic $[Cu(L)_2]^+$ coordination entity unit, the copper ion is tetracoordinated, and its coordination sphere is formed by four nitrogen atoms, two from pyridyl rings, and two from imino groups, all provided by two bidentate ligands. As in coordination entity **1**, the small bite angle of the ligand **L**, resulted in two N–Cu–N of 80.94(18)°, values that are not typical for a tetrahedral geometry. This fact as well as the steric hindrance caused by the bulky **L** ligand lead to important distortion of the tetrahedral environment of the copper (I) ion (see angle values in

ACCEPTED MANUSCRIPT

table 2).[30] Moreover, these geometric restraints can also explain the difference in the values of the dihedral angle between the least-square planes of the pyrene fragment and NN-chelate iminopyridine fragment in the two coordination entities, 56.54° in **1**, and 43.94° in **2**. The lengths of the two Cu–N bonds are very close (Cu1—N1 2.041(4) Å and, Cu1—N2 2.090(4) Å), and, as in coordination entity **1**, the formal double bond character in the imino fragment is maintained (C6–N2 1.275(7) Å).

The crystal packing of coordination entity **2** (Fig. S4) revealed the presence of two sets of short contacts, C–H···F and C–H···π. More precisely, the non-coordinating anions of BF_4^- are involved in hydrogen bonding (see values in table 3), which interconnects the cationic coordination entity units into supramolecular layers parallel with the *ac* crystallographic plane, while the aromatic rings within the $[Cu(L)_2]^+$ units establish numerous C–H···π contacts in the three directions of the crystal. Each of the two aromatic fragments, namely, the pyridyl and pyrene fragments, connects to neighboring $[Cu(L)_2]^+$ units, *via* C–H···π contacts, into 2D networks developing in different directions (as highlighted in Fig. 5), thus generating a 3D supramolecular net. In addition coordination entity **2** forms over 40 specific interactions between the 6-membered rings[28] (Table S3).

Table 3. Geometry of intermolecular interactions (distances in Å and angles in °) in **2** and **3**.

*Cg*1, *Cg*2, *Cg*3, *Cg*4 and *Cg*5 are the centers of gravity of the N1/C1÷C5; C17÷C19/C21÷C23; C7÷C10/C21/C22; C13÷C17/C23 and, respectively C10÷C13/C22/C23 in coordination entity **2**.

*Cg*1, *Cg*2, *Cg*3, and *Cg*4 are the centers of gravity of the C7÷C12; C11/C12/C16/C20÷C22; C10/C11/C13÷C16; and, respectively C15÷C20 in coordination entity **3**.

D–H···A	d(D···H)	d(H···A)	d(D ···A)	<(DHA)
coordination entity **2**				
C3–H3···F1^{i}	0.93	2.54	3.3702(2)	148.79

ACCEPTED MANUSCRIPT

C3–H3···F1^{ii}	0.92	2.54	3.1738(88)	110.44
C8–H8···F2A^{iii}	0.93	2.63	3.5543(2)	168.35
C6–H6···F2B^{iv}	0.93	2.61	3.2057(2)	122.21
C14–H14···F1^{v}	0.93	2.51	3.3550(118)	149.66
C9–H9···*Cg*1^{ii}	0.93	2.91	3.5369(68)	125.14
C15–H15···*Cg*1^{vi}	0.92	3.60	4.3225(103)	135.56
C11–H11···*Cg*2^{ii}	0.93	3.24	3.7631(99)	117.59
C1–H1···*Cg*2^{vii}	0.93	3.58	4.2281(70)	128.51
C2–H2···*Cg*2^{vii}	0.93	3.40	4.1282(66)	136.71
C11–H11···*Cg*3^{ii}	0.93	3.26	3.5680(83)	101.42
C12–H12···*Cg*3^{ii}	0.92	2.99	3.4026(101)	108.34
C1–H1···*Cg*3^{vii}	0.93	3.13	4.0404(70)	165.83
C2–H2···*Cg*4^{viii}	0.93	3.35	4.0110(59)	129.43
C6–H6···*Cg*4^{ix}	0.92	3.50	4.0989(65)	124.51
C1–H1···*Cg*5^{viii}	0.93	2.66	3.4019(64)	136.33
C2–H2···*Cg*5^{viii}	0.93	3.60	3.8917(66)	101.07
C11–H11···*Cg*5^{ix}	0.93	3.42	4.2105(91)	144.15
coordination entity **3**				
C18–H18···O2^{i}	0.92	2.61	3.3520(98)	136.51
C22–H22···O3^{ii}	0.93	2.70	3.5901(72)	157.99

ACCEPTED MANUSCRIPT

C6–H6···Cl1^{iii}	0.93	2.76	3.5790(61)	146.97
C2–H2···Cl1^{iii}	0.93	2.75	3.5680(62)	146.58
C8–H8···*Cg*2^{iv}	0.93	3.40	3.6776(63)	99.63
C9–H9···*Cg*3^{iv}	0.92	3.18	3.8686(64)	131.63

- Symmetry transformations used to generate atoms in coordination entity **2**: i) 1-x, y, 1-z; ii) x, y, z; iii) x, -1+y, z; iv) 1-x, -1+y, 1-z; v) 0.5-x, -1.5+y, -z ; vi) 0.5+x, 0.5+y, 1+z ; vii) -0.5+x, 1.5+y, z ; viii) 1-x, 1+y, -z ; ix) 1.5-x, 0.5+y, -z.
- Symmetry transformations used to generate atoms in coordination entity **3**: i) -x, -y, 1-z; ii) -0.5+x, -y, 0.5-z; iii) -0.5+x, 0.5-y, z; iv) 0.5+x, 0.5-y, z.

Single crystals of **3** were obtained by recrystallization from acetone/hexane and the crystal structure determination revealed a mononuclear coordination entity described by the formula: [Re(L)$(CO)_3$Cl] **3** (Fig. 4). Selected parameters of the X-ray diffraction data collection and refinement are gathered in Table 1. The compound crystallizes in the orthorhombic system, in a centrosymmetric space group *Pcab*.

ACCEPTED MANUSCRIPT

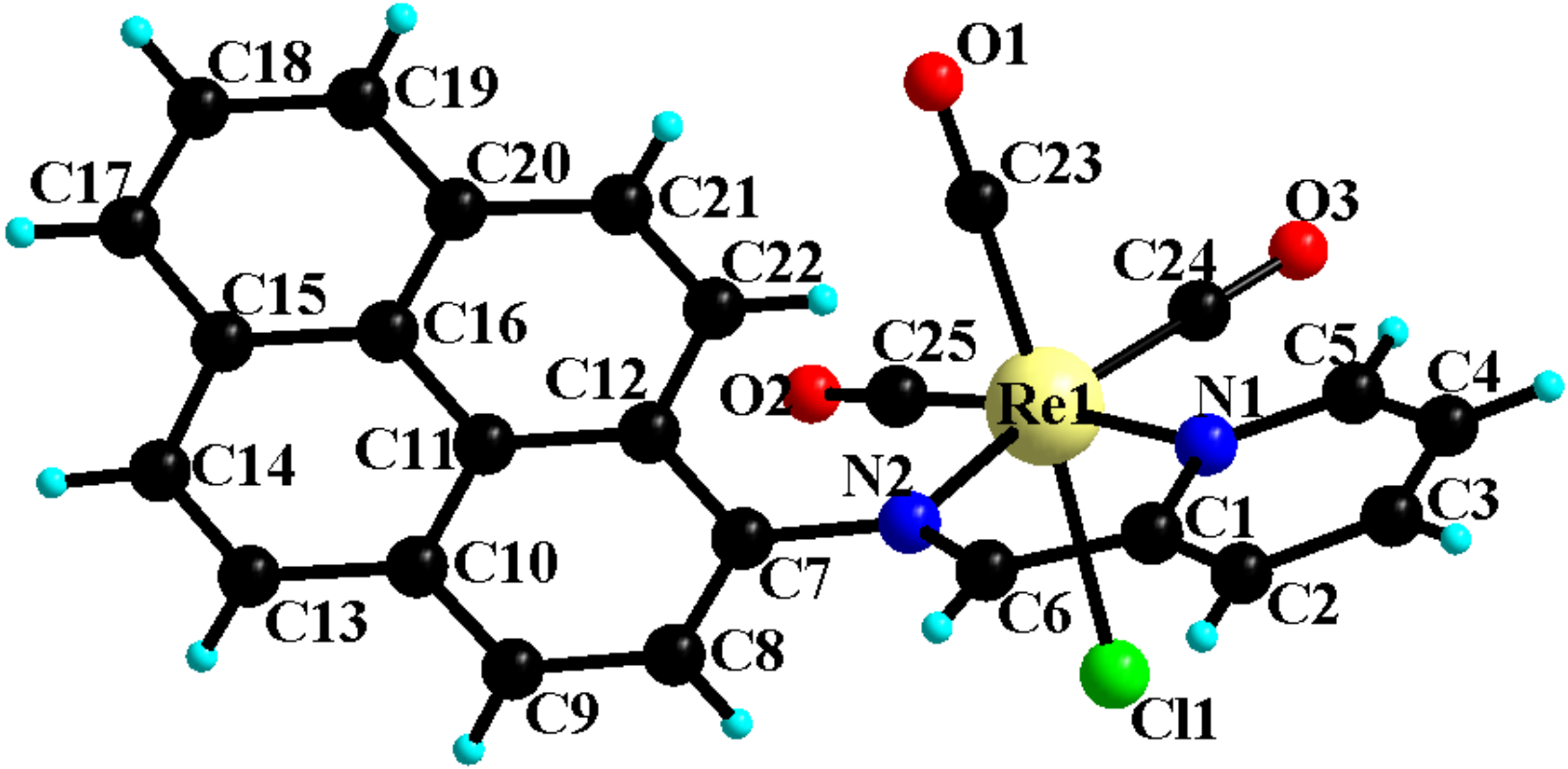

Fig. 4 Crystal structure of coordination entity **3** with atom numbering scheme.

ACCEPTED

ACCEPTED MANUSCRIPT

Within the coordination entity, the rhenium center is surrounded by the bidentate chelating **L** ligand, three carbonyl ligands arranged in a facial fashion, and a chlorine atom and its coordination sphere present the expected although slightly distorted octahedral geometry. This minor distortion is caused by the steric requirements associated with the presence of ligands of different nature. Thus, around the Re(I) ion, the values corresponding to *cis* angles (see table 2) are very close to the ideal value of 90°, except the N–Re1–N angle with the significantly lower value of 74.21(17)° as imposed by the small bite distance of a α-iminopyridyl type ligand. In ligand **L**, the dihedral angle between the least-square planes of the pyrene fragment and iminopyridyl fragment is 84.35°, a value significantly larger than the ones observed for the other two coordination entities. The length of the two Re–N bonds is identical (2.177(4) Å), and the formal double bond character in the imino fragment is maintained (C6–N2 1.283(6) Å). All three Re–CO bond lengths are very close, and the Re–C–O angles present minor deviations from linear structure, values ranging from (174.5(5)° to 177.7(5)°). Similar bond lengths and angle values have been observed in related rhenium (I) systems.[26]

In the crystal, the ligands surrounding the Re(I) ion are involved in two sets of interactions: hydrogen bonding and $\pi\cdots\pi$ stacking. Thus, each two of the three CO ligands establishes short C–H···O contacts (H18···O2 2.61 Å; H22···O3 2.70 Å) with hydrogen atoms from pyrene fragments linking neighboring molecules into layers parallel with the *ac* crystallographic plane (Fig. S5). These layers are interconnected into a 3D network through hydrogen bonds formed between the chlorine atom and hydrogen atoms from the pyridine ring (H2···Cl1 2.75 Å), and the imino group (H6···Cl1 2.76 Å) as depicted in Fig. S6.

Furthermore, viewing along the crystallographic *a* axis, one can observe columns formed by pyrene fragments linked alternatively *via* C–H$\cdots\pi$ (C8–H8$\cdots$*Cg*2 3.40 Å; C9–H9$\cdots$*Cg*3 3.18 Å) and, respectively $\pi\cdots\pi$ interactions (*Cg*3$\cdots$ *Cg*4 3.78 Å) as shown in Figure S7. This zipper-like arrangement of the pyrene fragments is also observed in coordination entity **1** (Fig. S3). Note that coordination entity **3** forms over 40 specific interactions between the 6-membered rings[28] (Table S4).

Determination of the thermodynamic parameters controlling the equilibria

ACCEPTED MANUSCRIPT

Since the formation of coordination entities **1** and **2** was accompanied by a strong color change, UV-absorption spectroscopy was used to determine the corresponding binding constants. Therefore, ligand **L** was titrated with a solution of the selected metal ion. To ensure the solubility of the ligand, the metal ions and the coordination entities, these measurements were performed in 1:1 mixtures of acetonitrile and dichloromethane. Fig. 5 shows the formation of **1** is associated to the appearance of an absorption band centered at 445 nm. Knowing that **1** displays a 1:1 stoichiometry, a non-linear curve fitting process allowed us to estimate the apparent binding constant $K_1 = 1.3\ 10^5$. At this stage, one should note the equilibria involving zinc salts and iminopyridine-based ligands are most often not studied in a quantitative manner.[29,31]

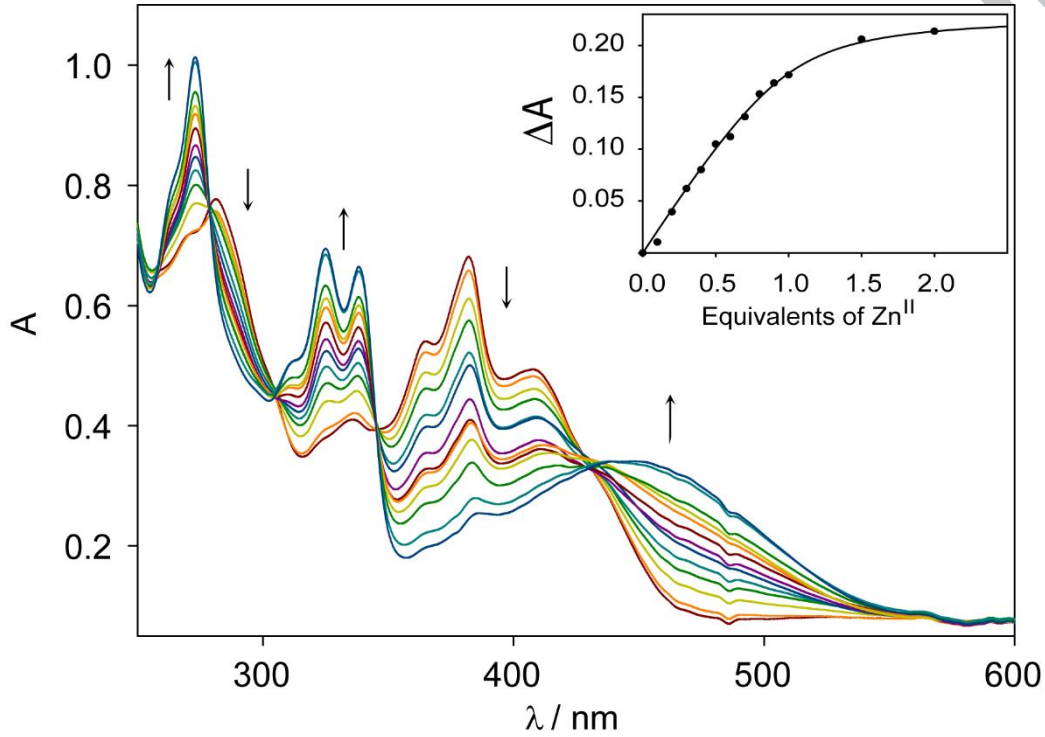

ACCEPTED MANUSCRIPT

Fig. 5 Evolution of the UV-vis absorption spectrum upon addition of zinc (II) chloride over a solution of ligand **L** ($C = 10^{-5}$ M, CH_2Cl_2/CH_3CN (1/1)); *inset*: evolution of the absorbance at λ = 460 nm upon addition of Zn(II) and curve obtained with fitted parameters

coordination entity **2** was studied in the same conditions (solvent, concentrations), however no significant modification of the spectrum was observed, despite the addition of copper (I) up to two equivalents. This behavior which suggests a rather small binding constant prompted us to consider another technique to determine the binding constant associated with the formation of coordination entity **2**, namely isothermal titration calorimetry (ITC). Moreover, this technique allows a straightforward determination of other thermodynamic parameters (ΔH, ΔS) and to confirm the stoichiometry of the coordination entities under study. At this stage, one should also note that, to the best of our knowledge, this ITC study is the first one led either with iminopyridine-based ligands or copper (I) salts. As a consequence, this work constitutes an interesting first step towards a better understanding of their coordination chemistry. This study could not be performed with Re(I) metal cation since heating is needed and CO gas is released during the reaction.

In order to probe the reliability of our titration methods, coordination entity **1** was first studied by ITC. Thermodynamic parameters and standard deviations were determined according to three independent experiments by fitting experimental data with equation 1. The thermodynamic parameters determined in this manner ($K_1 = (1.36 \pm 0.14)\ 10^5$, n = 1.09) proved to be in good agreement with the ones obtained from UV-visible spectroscopy and the 1:1 stoichiometry was confirmed (n=1) (Fig. 6). On this ground, similar measurements were led with ligand **L** and $Cu(CH_3CN)_4BF_4$ in the same conditions. The tetrakis(acetonitrile)copper(I) coordination entity appeared as a relevant candidate since it displays easily exchangeable ligands. The corresponding experiments demonstrate ligand **L** also forms a CuL_2 coordination entity in this mixture of solvents and afford the corresponding thermodynamic parameters (see Table 4). A first assessment lies on the relatively weak interaction between the copper center and the ligand as compared with the zinc coordination entity. Indeed, the determined binding constant proved to be two orders of magnitude smaller with the copper salt in these conditions, despite the initial presence of labile acetonitrile ligands.

ACCEPTED MANUSCRIPT

Both metals exist as coordination entities with acetonitrile molecules in these solutions, most likely $[Cu(CH_3CN)_4]^+$ and $[ZnCl_2(CH_3CN)_2]$ (Equation 3).[32] As a consequence, the establishment of ligand-metal coordination bonds requires the release of acetonitrile molecules (Equation 4). The formation of $[Cu\mathbf{L}_2]$ is favored by only 2.7 kJ.mol^{-1} compared to the $[Zn\mathbf{L}Cl_2]$. However, a striking difference appears when considering the entropic contributions. The zinc (II) coordination entity is formed with a positive entropy ($-T\Delta S = -1.4$ kJ.mol^{-1}), which is expected since two acetonitrile molecules are released upon complexation of the bidentate ligand. However, the complexation of copper (I) by **L** is significantly limited by a negative entropic parameter ($-T\Delta S = 8.2$ kJ.mol^{-1}), although four acetonitrile molecules are released during this reaction. This unexpected assessment may lie on experimental conditions, such as the solvent or the ionic strength, or could result from the large steric hindrance around $Cu\mathbf{L}_2$.

$$Q = \frac{n\,L_t\,\Delta H\,V_0}{2}\left[1 + \frac{M_t}{n\,L_t} + \frac{1}{n\,K\,L_t} - \sqrt{\left(1 + \frac{M_t}{n\,L_t} + \frac{1}{n\,K\,L_t}\right)^2 - \frac{4\,M_t}{n\,L_t}}\right] \quad (1)$$

$$m\ \mathbf{L} + M \rightleftharpoons \mathbf{L}_m M \quad (2)$$

$$n\ \mathbf{CH_3CN} + M \rightleftharpoons M(CH_3CN)_n \quad (3)$$

$$M(CH_3CN)_n + m\ \mathbf{L} \rightleftharpoons \mathbf{L}_m M + n\ \mathbf{CH_3CN} \quad (4)$$

ACCEPTED MANUSCRIPT

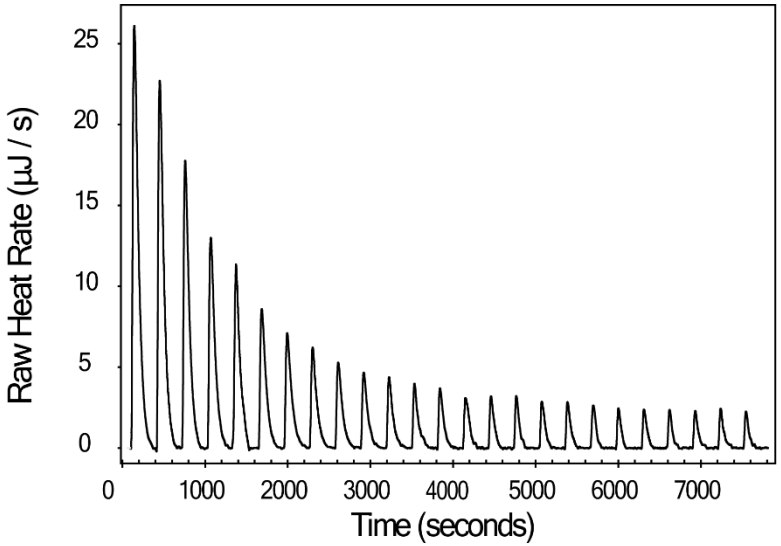

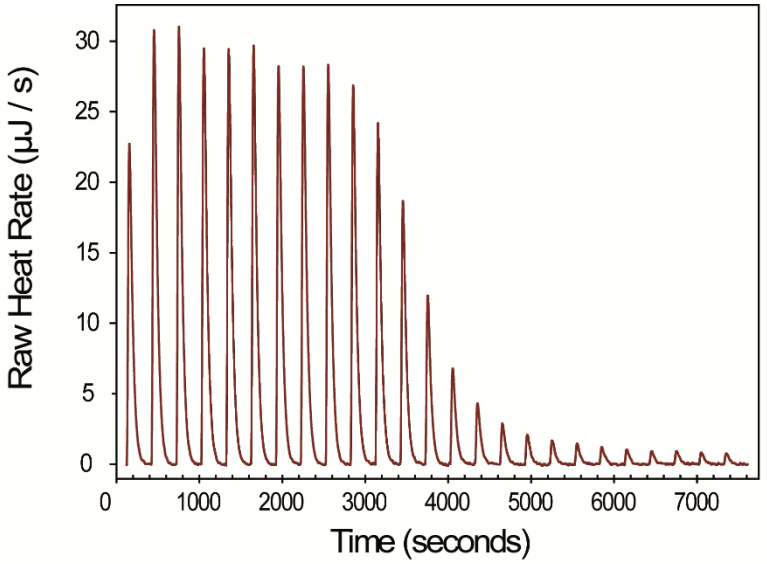

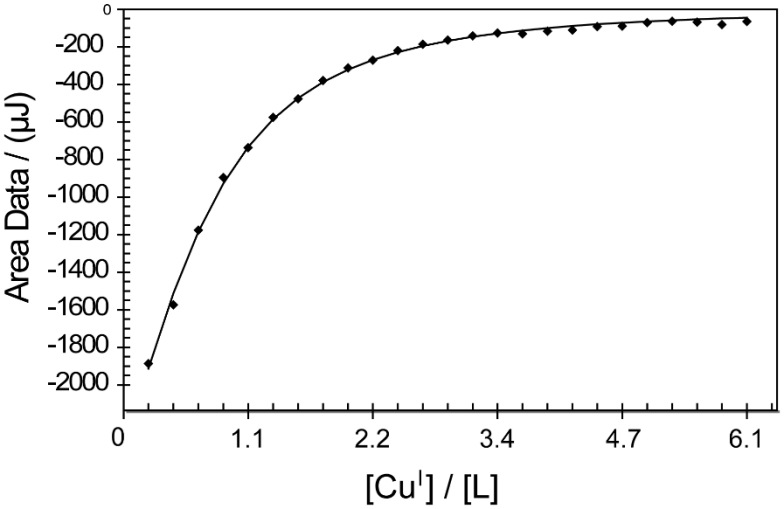

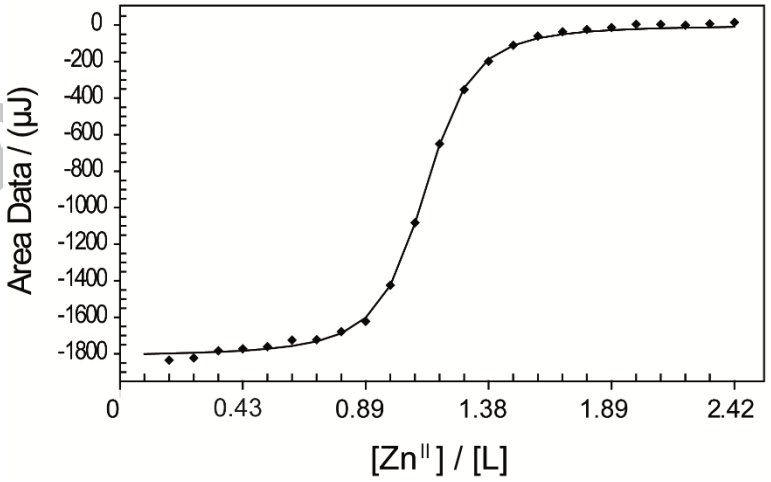

ACCEPTED MANUSCRIPT

Fig. 6a Titration of ligand **L** (1 mM) by $Cu(CH_3CN)_4BF_4$ (20 mM) in mixture of CH_2Cl_2/CH_3CN = 1/1 (*v/v*)

Fig. 6b Titration of ligand **L** (1 mM) with $ZnCl_2$ (8 mM) in CH_2Cl_2/CH_3CN = 1/1 (*v/v*)

(V_{cell} = 0.950 µL; V_{inj} = 10 µL; stirring speed: 250 rpm; T = 25°C) – Heats were respectively corrected by subtracting the contribution corresponding to the dilution of the tetrakis(acetonitrile)copper (I) tetrafluoroborate and zinc chloride solutions.

Table 4. Thermodynamic parameters determined by isothermal titration calorimetry.

Coordination entity	ΔH (kJ.mol^{-1})	–T.ΔS (kJ.mol^{-1})	ΔG (kJ.mol^{-1})	K_a
$[Cu(\mathbf{L})_2]BF_4$	–26.0 ± 2.5	8.2 ± 3.0	–17.8 ± 0.5	2.15 (± 0.87) 10^3
$[Zn\mathbf{L}Cl_2]$	–28.7 ± 0.2	–1.4 ± 0.3	–30.0 ± 0.5	1.82 (± 0.37) 10^5

Optical properties

Electronic absorption spectra of ligand **L** and coordination entities **1-3** were recorded in dichloromethane solution (Fig. 7). Ligand **L** exhibits well-separated vibronic bands located at 357, 375 and 402 nm. The red shift of these vibronic bands in comparison to pyrene results from the interaction between the pyrene and the iminopyridine fragments, as previously observed for pyrenebipyridine ligands.[33] In coordination entities **1, 2** and **3**, in addition to the intraligand (IL) π→π* transitions around 275 nm, pyrene vibronic bands between 300 and 400 nm are observed. Broad bands located around 465 nm for zinc coordination entity **1** and 425 nm for coordination entity **2** are attributed to the red shift of the intramolecular charge transfer (ICT). This results from the interaction between the pyrene unit and the electron deficient iminopyridine unit, because of the Lewis acidity nature of the metal cations.[25] As for coordination entity **3**, the band located around 450 nm might the combination of the ICT and the metal to ligand charge transfer (Re(dπ) → ligand(π*) ^{1}MLCT transition.[34]

ACCEPTED MANUSCRIPT

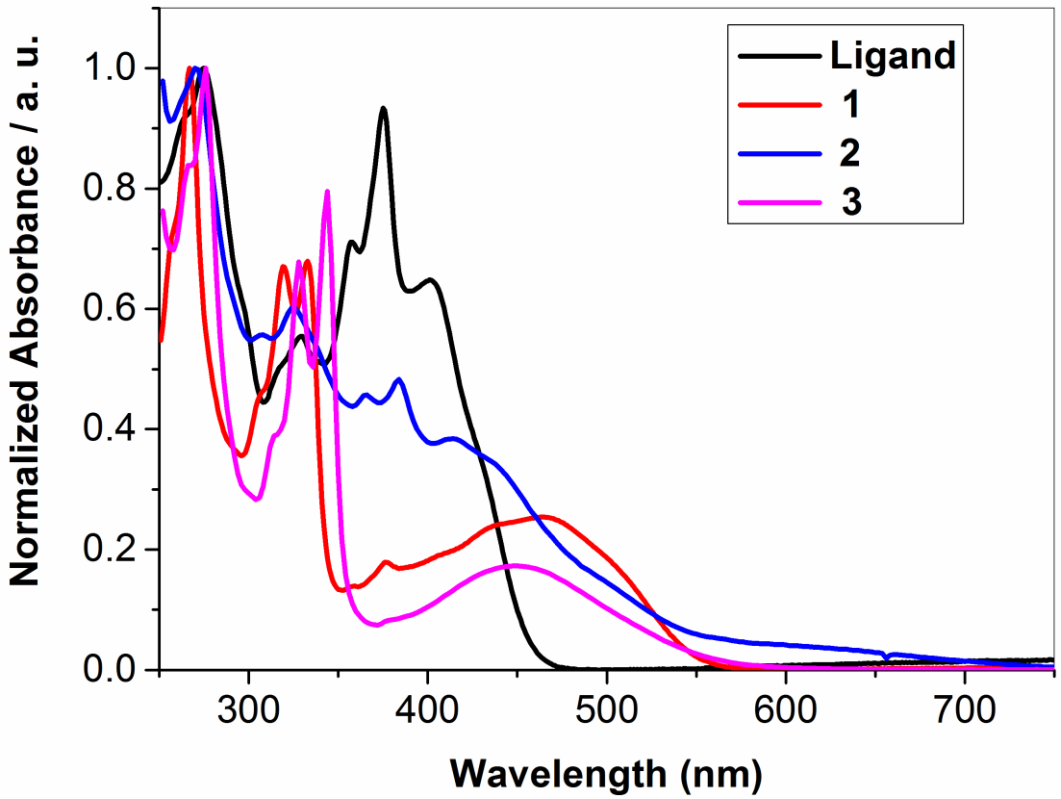

Fig. 7 UV-Visible absorption spectra of ligand **L** and coordination entity **1**-**3** in dichloromethane (C = 10^{-5} M).

All fluorescence quantum yields and optical data are summarized in Table 5. Measurements were performed in dichloromethane in order to prevent coordination entity dissociation (this phenomenon was observed in acetonitrile or methanol for instance). In solution, ligand **L** (Fig. S8) and the corresponding zinc **1** (Figure S9), copper **2** (Figure S10) and rhenium **3** (Figure S11) coordination entities give emission maxima around

ACCEPTED MANUSCRIPT

412-414 nm. Single photon-timing measurements (Table 5) reveal that all compounds mainly give mono-exponential decay kinetics in CH_2Cl_2 solution except for coordination entity **2**. In the latter case, the longest lifetime at about 20 ns with minor contribution of 2% may be attributed to the MLCT structure in the coordination entity. [34]

Altogether, these measurements are in agreement with a monomer-type pyrene emission since the excimer state of pyrene derivatives produces fluorescence at much longer wavelengths (between 450 and 520 nm) with lifetimes about 150-300 ns. [6b,35,36] While ligand **L** and coordination entity **1** present high fluorescence quantum yield, coordination entities **2** and **3** in CH_2Cl_2 solution display similar emission spectra but much lower fluorescence quantum yields. Since copper (I) and rhenium (I) metals can be involved in metal-to-ligand charge transfers (MLCT), the relaxation pathways are apparently modified, explaining why deexcitation mainly occurs in a non-radiative manner.[34]

In the solid-state, visible absorption bands of ligand **L** are bathochromically shifted by 35 nm. The planarization of the molecule in the solid state may be an explanation for an increased charge transfer from the pyrene to the pyridyl ring.[37] As for coordination entities, their UV-vis absorption spectra are not significantly changed in the solid state. Coordination entity **1**, which only includes one pyrene unit, displays a typical pyrene monomer emission, as in solution. Its crystal structure shows a poor overlap between pyrene rings, which probably results from the rigid molecular skeleton and explains the observed monomer type emission.[18] Analyzing the behavior of the three coordination entities **1-3**, it is also worth noting coordination entities **2** and **3** display neither monomer nor excimer emission in the solid state. Such a fluorescence quenching is common in the solid state because non-radiative relaxation is generally favored when short distances separate neighboring chromophores. [38]

Table 5. Long wavelength absorptions (λ/nm), emission maxima (λ_{em}/nm), fluorescence quantum yields (Φ_F), fluorescence decay times (τ_f/ns) and their % intensity contributions (given in brackets) of ligand **L** and coordination entities **1-3** in CH_2Cl_2 solution and on thin films at 25 °C (λ_{exc} = 317 nm).

Compound	Methylene chloride	Thin Film

ACCEPTED MANUSCRIPT

	λ	λ_{em}	Φ_F [a]	$\tau_{f(1)}$	$\tau_{f(2)}$	λ	λ_{em}
Ligand L	412	414	0.21	4.35	-	447	409
Compound 1	465	412	0.29	4.32	-	467	400
Compound 2	440	412	0.018	4.16 (98)	20.0 (2)	445	nd
Compound 3	448	413	0.071	4.39	-	446	nd

[a] *Fluorescence quantum yields have been calculated with respect to fluorescence emission of pyrene standard (λ_{exc} = 317 nm, Φ_F = 0.32, in cyclohexane).*[39] *nd: not determined*

Conclusions

A hybrid ligand **L** which associates an emissive pyrene fragment and an iminopyridine coordinating unit has been prepared using a straightforward synthetic strategy. This ligand was reacted with different transition metal ions and three coordination entities (**1-3**) have been prepared and fully characterized including X-ray structure determination. Reaction of ligand **L** with one equivalent of $ZnCl_2$ or one equivalent of $[Re(CO)_5Cl]$ resulted in the formation of neutral coordination entities $[ZnLCl_2]$, **1** or $[ReLCl(CO)_3]$, **3** while the reaction with half equivalent of copper (I) afforded a charged $[CuL_2]^+$, **2**. The photophysical studies of these compounds show clearly a different behavior depending on the metal ion used. In fact, using zinc (II) ion resulted in a quasi identical behavior as the free ligand while using copper (I) and rhenium (I) resulted in a decrease of the monomer emission of pyrene as compared with the free ligand. Thus, the results obtained in this work can contribute to the design of novel sensors for metal ions based on pyrene fragment and iminopyridine coordinating unit. Further investigations including the preparation of novel pyrene-alkyl-iminopyridine ligands as well as the doubly substituted ligands with the pyrene as well as a mixture of fluorophores are currently in progress in our laboratory.

ACCEPTED MANUSCRIPT

Appendix A. Supplementary data

CCDC 1452985, 1012506 – 1012508 contain the supplementary crystallographic data for <Ligand L, coordination entities 1, 2 and 3>. These data can be obtained free of charge via http://www.ccdc.cam.ac.uk/conts/retrieving.html, or from the Cambridge Crystallographic Data Centre, 12 Union Road, Cambridge CB2 1EZ, UK; fax: (+44) 1223-336-033; or e-mail: deposit@ccdc.cam.ac.uk.

References

1 A. Laurent, *Ann. Chim. Phys.*, 1837, **66**, 136-213.

2 J.I. Wu, M.A. Dobrowolski, M.K. Cyrański, B.L. Merner, G.J. Bodwell, Y. Mo, P.V.R. Schleyer, *Mol. Phys.*, 2009, **107**, 1177-1186.

3 (a) C. Ehli, G. M. Aminur Rahman, N. Jux, D. Balbinot, D. M. Guldi, F. Paolucci, M. Marcaccio, D. Paolucci, M. Melle-Franco, F. Zerbetto, S. Campidelli, M. Prato, *J. Am. Chem. Soc*., 2006, **128**, 11222-11231; (b) D. Canevet, A. Pérez del Pino, D. B. Amabilino, M. Sallé, *J. Mater. Chem*., 2011, **21**, 1428-1437; (c) D. Canevet, A. Pérez del Pino, D. B. Amabilino and M. Sallé, *Nanoscale*, 2011, **3**, 2898-2902.

4 (a) F. Moggia, C. Videlot-Ackermann, J. Ackermann, P. Raynal, H. Brisset, F. Fages, *J. Mater. Chem*., 2006, **16**, 2380-2386; (b) K.-C. Wu, P.-J. Ku, C.-S. Lin, H.-T. Shih, F.-I. Wu, M.-J. Huang, J.-J. Lin, I.-C. Chen, C.-H. Cheng, *Adv. Funct. Mater*. 2008, **18**, 67-75; (c) J. Kwon, J.-P. Hong, S. Lee, J.-I. Hong, *New J. Chem*., 2013, **37**, 2881-2887; (d) H.-Y. Oh, C. Lee, S. Lee, *Org. Electron*., 2009, **10**, 163-169; (e) T. M. Figueira-Duarte, K. Müllen, *Chem. Rev*., 2011, **111**, 7260-7314; (f) J. Kwon, J.-P. Hong, S. Noh, T.-M. Kim, J.-J. Kim, C. Lee, S. Lee, J.-I. Hong, *New J. Chem*., 2012, **36**, 1813-1818; (g) J.-W. Mun, I. Cho, D. Lee, W. S. Yoon, O. K. Kwon, C. Lee, S. Y. Park, *Org. Electron*., 2013, **14**, 2341-2347; (h) O. P. Lee, A. T. Yiu, P. M. Beaujuge, C. H. Woo, T. W. Holcombe, J. E. Millstone, J. D. Douglas, M. S. Chen, J. M. J. Fréchet, *Adv. Funct. Mater*. 2011, **23**, 5359-5363; (i) J. Kwon, T.-M. Kim, H.-S Oh, J.-J. Kim, Jong-In Hong, *RSC Adv*., 2014, **4**, 24453-24457.

ACCEPTED MANUSCRIPT

5 (a) J. Fernández-Lodeiro, C. Núñez, C. S. de Castro, E. Bértolo, J. S. Seixas de Melo, J. L. Capelo, C. Lodeiro, *Inorg. Chem*., 2013, **52**, 121-129; (b) M. C. González, F. Otón, R. A. Orenes, A. Espinosa, A. Tárraga, P. Molina, *Organometallics*, 2014, **33**, 2837-2852; c) E. Brunetti, J.-F. Picron, K. Flidrova, G. Bruylants, K. Bartik, I. Jabin, *J. Org. Chem*., 2014, **79**, 6179-6188.

6 (a) J. B. Birks *Photophysics of Aromatic Molecules*; John Wiley: New York, 1970; Chapter 7; (b) F. M. Winnik, *Chem. Rev*., 1993, **93**, 587-614.

7 (a) A. P. de Silva, H. Q. N. Gunaratne, T. Gunnlaugsson, A. J. M. Huxley, C. P. McCoy, J. T. Rademacher, T. E. Rice, *Chem. Rev*., 1997, **97**, 1515-1566; (b) K. Rurack, U. Resch-Genger, *Chem. Soc. Rev*. 2002, **31**, 116-127.

8 (a) J. A. Simon, S. L. Curry, R. H. Schmehl, T. R. Schatz, P. Piotrowiak, X. Jin, R. P. Thummel, *J. Am. Chem. Soc*., 1997, **119**, 11012-11022; (b) A. Del Guerzo, S. Leroy, F. Fages, R. H. Schmehl, *Inorg. Chem*., 2002, **41**, 359-366, (c) S. Leroy, T. Soujanya, F. Fages, *Tetrahedron Lett*., 2001, **42**, 1665-1667; (d) S. Leroy-Lhez, F. Fages, *Eur. J. Org. Chem.*, 2005, 2684-2688.

9 (a) J. F. Michalec, S. A. Bejune, D. R. McMillin, *Inorg. Chem.*, 2000**, 39**, 2708-2709; b) X. Peng, Y. Xu, S. Sun, Y. Wu, J. Fan, *Org. Biomol. Chem.*, 2007, ***5***, 226-228; c) A. C. Benniston, A. Harriman, D. J. Lawrie, A. Mayeux, *Phys. Chem. Chem. Phys*., 2004, **6**, 51-57.

10 B. Bodenant, F. Fages, M.-H. Delville, *J. Am. Chem. Soc.*, 1998, **120**, 7511-7519.

11 A. Harriman, M. Hissler, R. Ziessel, *Phys. Chem. Chem. Phys*., 1999, **1**, 4203-4211.

12 H. Shirase, Y. Mori, Y. Fukuda, M. Uchiyama, *Monatsh. Chem*., 2009, **140**, 801-805.

13 R.A. Allão Cassaro, J.R. Friedman, P.M. Lahti, *Polyhedron*, 2016, **117**, 7-13

14 (a) C. Piguet, G. Bernardinelli, G. Hopfgartner, *Chem. Rev*. 1997, 97, 2005-2062; (b) R. Ziessel, A. Harriman, A. El-Ghayoury, L. Douce, E. Leize, H. Nierengarten, A. Van Dorsselaer, *New J. Chem*., 2000, **24**, 729-732; (c) M. C. Young, A. M. Johnson, A. S. Gamboa, R. J. Hooley, *Chem. Commun.*, 2013, **49**, 1627-1629; (d) S. E. Howson, A. Bolhuis, V. Brabec, G.J. Clarkson, J. Malina, A. Rodger, P. Scott, *Nature Chem*., 2012, **4**, 31-36.

15 J. L. Bolliger, A. M. Belenguer, J. R. Nitschke, *Angew. Chem. Int. Ed*., 2013, **52**, 7958-7962.

16 R. A. Bilbeisi, T. K. Ronson, J. R. Nitschke, *Angew. Chem. Int. Ed*., 2013, **52**, 9027–9030.

17 (a) J. Cloete, S. F. Mapolie, *J. Mol. Catalysis A: Chemical*, 2006, **243**, 221-225; (b) P. Shejwalkar, N. P. E. B. RathBauer, *Dalton Trans*., 2011, **40**, 7617-7631; (c) S. Telitel, F. Dumur, D. Campolo, J. Poly, D. Gigmes, J. P. Fouassier, J. Lalevée, J. Polym. Sci., Part A: Polym. Chem. 2016, **54**, 702–713

18 (a) M. Licchelli, L. Linati, A. Orbelli Biroli, E. Perani, A. Poggi, D. Sacchi, *Chem. Eur. J*., 2002, **8**, 5161-5169; (b) M. Licchelli, A. Orbelli Biroli, A. Poggi, D. Sacchi, C. Sangermani, M. Zema, *Dalton Trans*., 2003, 4537-4545.

ACCEPTED MANUSCRIPT

19 (a) L. Zeng, E. W. Miller, A. Pralle, E. Y. Isacoff, C. J. Chang, *J. Am. Chem. Soc*., 2006, **128**, 10-11 ; (b) E. M. Nolan, S. J. Lippard, Acc. Chem. Res., 2009, **42**, 193-203.

20 Y-W. Dong, R-Q. Fan, P. Wang, L-G. Wei, X-M. Wang, H-J. Zhang, S. Gao, Y-L. Yang, Y-L. Wang, *Dalton Trans*., 2015, **44**, 5306-5322.

21 G. Canil, V. Rosar, S. Dalla Marta, S. Bronco, F. Fini, C. Carfagna, J. Durand, B. Milani, *ChemCatChem* , 2015, **7**, 14, 2255-2264

22 J. Sun, Z. Lu, Y. Li, J. Dai, *Journal of Thermal Analysis and Calorimetry*, 1999, **58**, 2, 383-391.

23 J. Dai, X-D. Yang, J-P. Sun, Z-R. Lu, M. Munakata, M. Maekawa, *Journal of Coordination Chemistry*, 1996, **38**, 4, 281-285.

24 G. M. Sheldrick, *Programs for the Refinement of Crystal Structures*, University of Göttingen, Göttingen, Germany, **1996.**

25 I. Guezguez, A. Ayadi, K. Ordon, K. Iliopoulos, D. G. Branzea, A. Migalska-Zalas, M. Makowska-Janusik, A. El-Ghayoury, B. Sahraoui, *J. Phys. Chem. C*, 2014, **118**, 7545-7553.

26 W. Liu, K. Heinze, *Dalton Trans.*, 2010, **39**, 9554-9564.

27 C. A. Hunter, J. K. M. Sanders, *J. Am. Chem. Soc.*, 1990, **112**, 5525–5534

28 R. Kruszynski, T. Sierański, *Cryst. Growth Des.*, 2016, **16**, 587–595.

29 T. S. Basu Baul, S. K., A. Linden, N. Raviprakash, S. K. Mannac, M. F. C. Guedes da Silva, *Dalton Trans*., 2014, **43**, 1191-1202.

30 S. Dehghanpour, N. Bouslimani, R. Welter, F. Mojahed, *Polyhedron*, 2007, **26**, 154-162.

31 (a) M. Schulz, M. Klopfleisch, H. Görls, M. Kahnes, M. Westerhausen, *Inorg. Chim. Acta*, 2009, **362**, 4706 4712; (b) J. J. Braymer, J.-S. Choi, A. S. DeToma, C. Wang, K. Nam, J. W. Kampf, A. Ramamoorthy, M. H. Lim, *Inorg. Chem*., 2011, **50**, 10724-10734; (c) J. J. Braymer, N. M. Merrill, M. H. Lim, *Inorg. Chim. Acta*, 2012, **380**, 26-268.

32 (a) G. J. Kubas, B. Monzyk, A. L. Crumbliss, (2007) Tetrakis(Acetonitrile)Copper(I) Hexafluorophosphate, in *Inorganic Syntheses*, Volume 19 (ed D. F. Shriver), John Wiley & Sons, Inc., Hoboken, NJ, USA. **2007**, doi: 10.1002/9780470132500. ch18; (b) J.C. Evans, G.Y.S. Lo, *Spectrochimica Acta*, 1965, **21**, 1033-1038.

33 T. Soujanya, A. Philippon, S. Leroy, M. Vallier, and F. Fages, *J. Phys. Chem. A*, 2000, **104**, 9408-9414;

34 R. N. Dominey, B. Hauser, J. Hubbard, J. Dunham, *Inorg. Chem*., 1991, **30,** 4754-4758.

35 (a) H. Nohta, H. Satozono, K. Koiso, H. Yoshida, J. Ishida, M. Yamaguchi, *Anal. Chem.*, 2000, **72**, 4199-4204; (b) E. J. Jun, H. N. Won, J. S. Kim, K.-H. Lee, J. Yoon, *Tetrahedron Lett*., 2006, **47**, 4577-4580.

36 M. J. Snare, P. J. Thistlethwaite, K. P. Ghiggino, *J. Am. Chem. Soc*., 1983, **105**, 3328-3332.

37 S. P. Wu, Z. M. Huang , S. R. Liu, P. K. Chung, *J Fluoresc.*, 2012, **22**, 1–7

ACCEPTED MANUSCRIPT

38 X. Ma, R. Sun, J. Cheng, J. Liu, F. Gou, H. Xiang, X. Zhou, *J. Chem. Educ*. 2016, **93**, 345−350

39 I. B. Berlman, "*Handbook of Fluorescence Spectra of Aromatic Molecules*" Academic Press, N.Y, **1971**.

ACCEPTED MANUSCRIPT

ACCEPTED MANUSCRIPT

Coordination entities of a Pyrene-based Iminopyridine ligand: Structural and photophysical properties

Awatef Ayadi,[a,b] Diana Branzea,[a] Magali Allain,[a] David Canevet,[a] Haluk Dinçalp,[c] Abdelkrim El-Ghayoury[a]*

We report herein a pyrene-based iminopyridine ligand **L** and its corresponding neutral (Zn(II) and Re(I)) and monocationic Cu(I) complexes, formulated as $[ZnLCl_2]$ **1**, $[ReLCl(CO)_3]$ **3** and $[CuL_2](BF_4)$ **2**. Photophysical studies of these compounds showed a monomer type pyrene emission and a higher fluorescence quantum yield for zinc complex **1** as compared with copper **2** and rhenium **3** complexes.

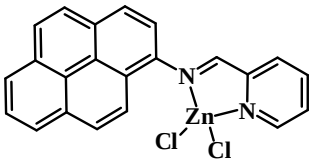

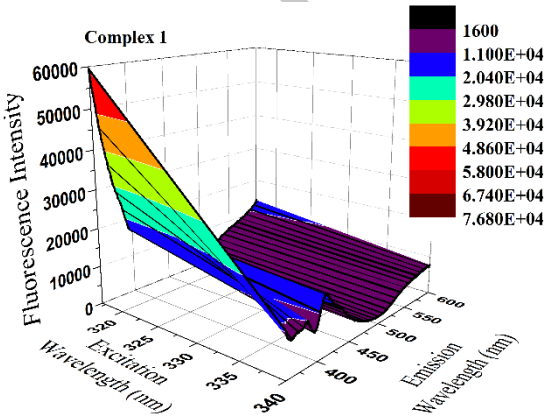

ACCEPTED MANUSCRIPT